ELSEVIER

Coordination Chemistry Reviews
208 (2000) 87–101

COORDINATION CHEMISTRY REVIEWS

www.elsevier.com/locate/ccr

Mechanisms of ultrafast metal–ligand bond splitting upon MLCT excitation of carbonyl-diimine complexes

Ian R. Farrell, Antonín Vlček Jr. *

Department of Chemistry, Queen Mary and Westfield College, University of London, London E1 4NS, UK

Received 17 August 1999; accepted 4 November 1999

Contents

Abstract

Using CO dissociation from $[Cr(CO)_4(bpy)]$, alkyl homolysis from $[Re(R)(CO)_3(dmb)]$ and dissociative isomerisation of $[Mn(Br)(CO)_3(^i Pr–DAB)]$ as characteristic examples, it is shown how excitation into charge transfer excited states can lead to ultrafast metal–ligand bond splitting. The overall course of organometallic photochemical reactions is clearly determined by excited state dynamics, which occur at the earliest times after excitation. Branching of the evolution of the optically prepared Franck–Condon excited state between reactive and relaxation pathways seems to be a general mechanism that limits photochemical quantum

* Corresponding author. Tel.: +44-020-7882-3260; fax: +44-020-7882-7794.
E-mail address: a.vlcek@qmw.ac.uk (A. Vlček Jr.).

PII: S0010-8545(99)00244-1

yields. CO dissociation and alkyl homolysis can be described as an adiabatic evolution on potential energy surfaces of metal-to-ligand charge transfer (MLCT) or sigma-bond-to-ligand charge transfer (SBLCT) excited states, respectively. These states acquire a dissociative character from upper states with which they interact along the reaction coordinate. Coupling of an excited state with the dissociative continuum of the electronic ground state provides an alternative reaction mechanism. This was demonstrated for the dissociative isomerisation of *fac*-[Mn(Br)$(CO)_3$(^{i}Pr–DAB)], which occurs from ligand-to-ligand charge transfer (LLCT) excited state. In general, it follows that an understanding of organometallic photochemistry requires a knowledge of the energies and characters of the relevant electronic states as a function of possible reaction coordinates.

Keywords: Photochemistry; Organometallics; Charge-transfer; Carbonyl; Diimine; Ultrafast dynamics; Bond splitting

1. Introduction

Traditionally, metal-to-ligand charge transfer, MLCT, and related excited states were believed to be rather unreactive with respect to metal–ligand bond splitting. However, recent studies, which were thoroughly reviewed by Vogler [1] and Vlček [2], have clearly demonstrated that very interesting photoreactivity can be induced by CT excitation. This includes: (i) dissociation of a 'spectator' ligand, usually CO; (ii) homolysis of a metal–alkyl or metal–metal bond in organometallic diimine complexes; and (iii) dissociative isomerisation of carbonyl-diimine complexes. The nature of the photoproducts, kinetics, and mechanisms of CT-induced photochemistry show a remarkable dependence on the structure of the photoactive species and on the medium. The rates of primary photoprocesses vary from a few hundred femtoseconds to several microseconds, that is over (at least) seven orders of magnitude! From a practical point of view, it is important to note that MLCT and related electronic transitions are often strongly allowed. Hence, charge transfer excitation represents a very efficient way to collect light energy.

While the reactivity of MLCT excited states is now a well established phenomenon, many puzzling mechanistic questions remain:

1. What really makes MLCT and similar excited states dissociative? Note, that bond dissociation from a MLCT state is largely counter-intuitive: MLCT excitation neither depopulates a strongly bonding orbital nor populates an antibonding one; moreover, the metal atom becomes a stronger Lewis acid and the ligand a stronger Lewis base.
2. Do the CT-induced bond splitting reactions involve nonradiative transitions to other, presumably ligand-field (LF), dissociative states or do they occur as smooth wave packet evolutions on the potential energy surfaces of optically prepared Franck–Condon states?
3. What structural factors determine the rates of bond splitting from CT excited states?

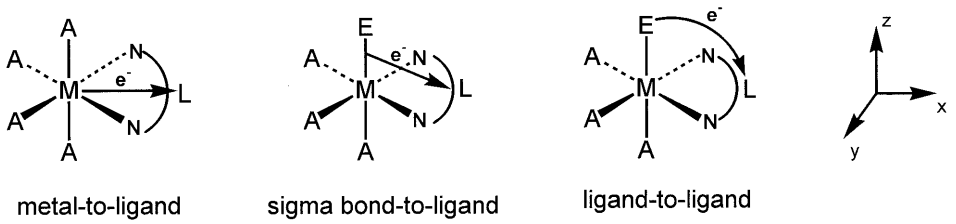

Fig. 1. Schematic representation of MLCT, LLCT, and SBLCT excited states. The axes orientation shown is used throughout this paper. NN represents a bidentate α-diimine ligand or, more generally, an electron acceptor L. MLCT: metal-to-ligand charge transfer; SBLCT: sigma-bond-to-ligand charge transfer; LLCT: ligand-to-ligand charge transfer. Note, that LLCT states are also called XLCT, if the excitation originates in a halide ligand. SBLCT states are often called σπ*, based on their orbital origin.

4. What structural factors and dynamic processes determine the quantum yields of bond splitting reactions from CT excited states?

In the course of our research, investigating the dynamics and mechanism of photochemical metal–ligand bond splitting, we have concentrated on the reactivity of MLCT, LLCT and SBLCT excited states, shown schematically in Fig. 1. Well known MLCT states originate in electron excitation from a metal d(π) orbital into an empty ligand-localised orbital, usually of a π* character. Other interesting reactive MLCT states like d(π)→σ*, described by Vogler [1,3], are not discussed herein. Ligand-to-ligand charge transfer, LLCT, excited states result from electron excitation from an occupied π orbital of one ligand into an empty π* orbital of another. On the other hand, sigma bond to ligand charge transfer (SBLCT) excited states (also known as σπ*) involve electron excitation from an orbital that is σ bonding, with respect to a metal–ligand bond, into a π* orbital localised on a *cis*-oriented, usually α-diimine, ligand. To understand the photobehaviour of CT-active complexes, it is important to note that MLCT, LLCT and SBLCT excited states often have the same symmetry. Hence, extensive mixing of orbitals (e.g. d(π)/ligand(π), σ/π*, etc.) and electronic states can occur [4–9]. Pure MLCT, LLCT or SBLCT states therefore represent only limiting cases. In most real molecules we encounter excited states of a more or less mixed character.

Herein, we shall discuss the early dynamics and resulting reactivity of excited states predominantly of MLCT, SBLCT and LLCT character, using $[Cr(CO)_4(bpy)]$, $[Re(R)(CO)_3(dmb)]$ and $[Mn(Br)(CO)_3(^iPr–DAB)]$ as archetypal respective examples (R = Me, Et; dmb = 4,4′-dimethyl-2,2′-bpy, $^iPr–DAB$ = *N*,*N*-bis-*iso*-propyl-1,4-diazabutadiene). Relevant experimental results have been described in detail elsewhere [10–12], so the following discussion will focus on more general, mechanistic aspects of these reactions and on their implications for organometallic photochemistry.

2. MLCT photochemistry: dissociation of an axial CO ligand from $[Cr(CO)_4(bpy)]$

Irradiation of $[Cr(CO)_4(bpy)]$ with visible light excites the Cr→bpy MLCT transition, triggering dissociation of an axial CO ligand [10,13–18]. The CO-loss

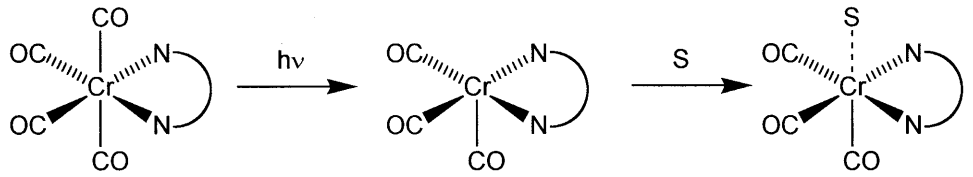

Fig. 2. The photochemistry of $[Cr(CO)_4(bpy)]$ induced by Cr → bpy MLCT excitation.

product immediately coordinates a solvent molecule, generating *fac*-$[Cr(L)(CO)_3(bpy)]$; L = solvent or a Lewis base molecule (e.g. phosphine) present in the solution, see Fig. 2. The quantum yield of CO dissociation decreases with decreasing excitation energy tuned over the range of the MLCT absorption band [17]. This observation, obtained under continuous irradiation, has clearly indicated that the reacting excited state keeps a memory of the original excitation energy. This implies that CO dissociation proceeds directly from the optically prepared ^{1}MLCT Franck–Condon excited state, prior to any relaxation. In full agreement with this conclusion, femtosecond time-resolved absorption spectra of $[Cr(CO)_4(bpy)]$ measured in pyridine or CH_2Cl_2 solutions have shown that the *fac*-$[Cr(S)(CO)_3(bpy)]$ photoproduct (S = solvent) is already produced within the first 400 fs [10]. Moreover, it follows that the photoproduct is formed concurrently with the population of two unreactive trapping states, presumably of ^{3}MLCT character. These two states decay to the ground state with lifetimes of 8 and 87 ps, respectively. The overall excited state dynamics of $[Cr(CO)_4(bpy)]$ are schematically shown in Fig. 3. Importantly, the relative values of the branching ratio between CO dissociation and relaxation were found to decrease with decreasing excitation energy in the same way as the photochemical quantum yield, Fig. 4. It follows that the overall photochemistry of $[Cr(CO)_4(bpy)]$, that is the nature of the products and quantum yield of the reaction, is determined at the very earliest times after excitation, that is within 400 fs.

The absence of any observable precursor to CO dissociation, together with its femtosecond rate, suggest that the potential energy surface of the reactive ^{1}MLCT state is unbound along the axial Cr–CO coordinate. Nevertheless, however well the femtosecond experiments have revealed the early excited state dynamics, they do not say anything about reasons for the ultrafast dissociative reactivity of the $[Cr(CO)_4(bpy)]$ ^{1}MLCT excited state. This question has been approached computationally by C. Daniel and D. Guillaumont who have calculated [19,20] potential energy curves of various excited states of $[Cr(CO)_4(bpy)]$ along the axial Cr–CO coordinate. Indeed, the calculated potential energy curve of the optically prepared $d_{xz} \rightarrow \pi^*$ MLCT excited state is dissociative, with only a very shallow minimum at an axial Cr–CO distance only a little longer than the equilibrium value. The physical reason for the dissociative character of this MLCT state has been revealed by an analysis of its wavefunction which showed a gradually increasing admixture of LF dissociative character along the reaction coordinate [20]. This computational result agrees with a qualitative explanation of the $[Cr(CO)_4(bpy)]$ photoreactivity

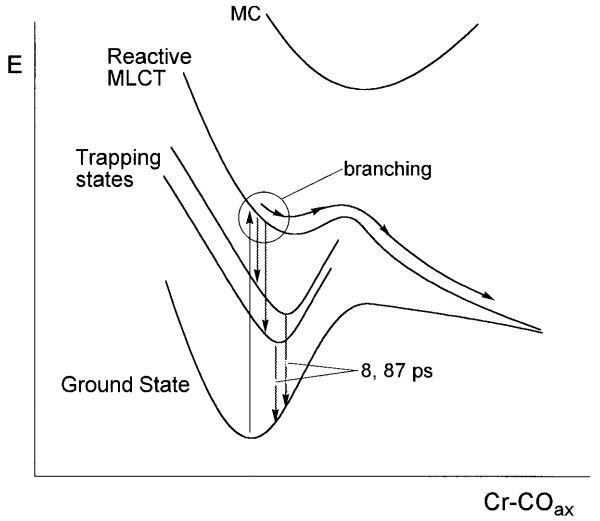

Fig. 3. The excited state dynamics of $[Cr(CO)_4(bpy)]$. Qualitative, idealised potential energy curves are used.

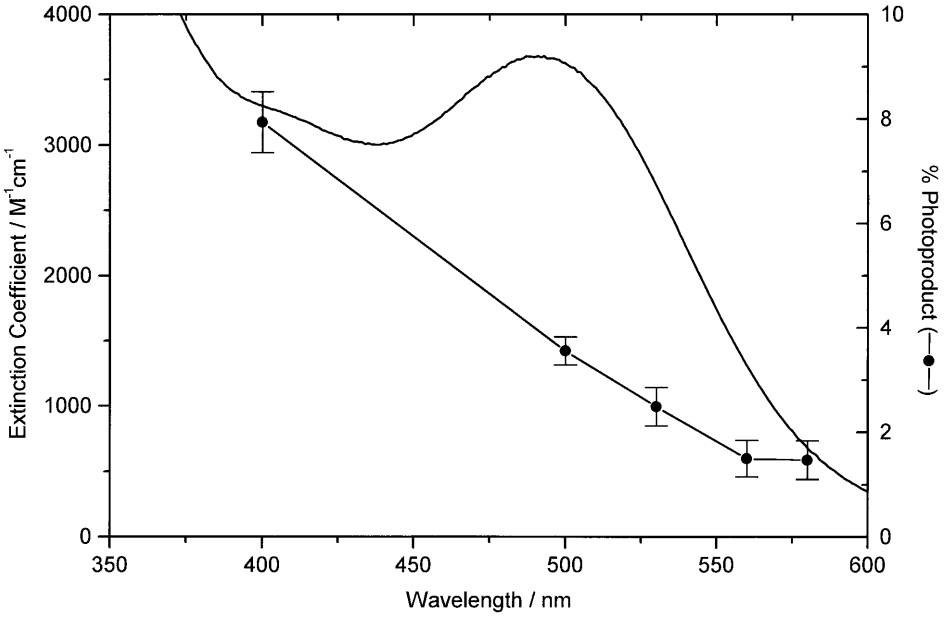

Fig. 4. Experimental evidence for branching between CO dissociation and relaxation to trapping states, as obtained for $[Cr(CO)_4(bpy)]$. Relative contribution of the $[Cr(S)(CO)_3(bpy)]$ photoproduct to the initially observed transient, which is related to the branching ratio, is shown (●) as a function of the excitation wavelength, together with the absorption spectrum of $[Cr(CO)_4(bpy)]$. See Ref. [10] for details.

based on vibronic mixing between MLCT and LF excited states [21]. (Note, that the mixing between these states becomes allowed as soon as the C_{2v} symmetry is broken by elongation of one of the two axial Cr–CO bonds).

One shouldn't be surprised that it is a spectator CO ligand that dissociates upon Cr→bpy MLCT excitation of [Cr(CO)$_4$(bpy)], and similarly, in other [22–24] carbonyl-diimine complexes. The $d_{xz} \rightarrow d_{z^2}$ MC excited state, which is strongly repulsive with respect to the axial Cr–CO bond, has the right symmetry to mix with the $d_{xz} \rightarrow \pi^*$ MLCT state upon asymmetric distortion of the axial OC–Cr–CO unit [21]. Also, CASSCF calculations have revealed that the CO ligands are not simply spectators with respect to MLCT excitation [25]. In fact, upon MLCT excitation, the electron density on the four CO ligands decreases more (by 0.426 electron) than on the Cr atom (0.357 electron). Furthermore, the axial CO ligands are depopulated more than the equatorial ones, by 0.262 and 0.164 electron, respectively. It follows that the MLCT excitation should be viewed as originating in the whole Cr(CO)$_4$ fragment instead at the Cr atom only.

Generally, it can be concluded that an MLCT excited state of carbonyl-diimine complexes can acquire a dissociative character by an interaction (avoided crossing) with a higher-lying repulsive LF state. This situation will occur in complexes in which the bonding between the metal atom and the dissociating ligand is rather short-range, its strength rapidly decreasing as the bond elongates. This is especially so in the case of metal carbonyls of first row transition metals, which have strong M→CO π-back bonding in the ground state.

3. SBLCT photochemistry: homolysis of a metal–alkyl bond in *fac*-[Re(R)(CO)$_3$(dmb)]

Previous studies [26–29] have clearly established that the formation of radicals by homolytic splitting of the Re–R bond in the complexes *fac*-[Re(R)(CO)$_3$(dmb)] is caused by irradiation into their lowest visible absorption band:

$$[\mathrm{Re(R)(CO)_3(\alpha\text{-diimine})}] \xrightarrow{h\nu,\ \mathrm{S}} [\mathrm{Re(S)(CO)_3(\alpha\text{-diimine})}]^{\bullet} + \mathrm{R}^{\bullet} \quad (1)$$

where S represents a solvent molecule. Similar photoreactivity was found for analogous Mn complexes [30], some [Ru(R)(X)(CO)$_2$(α-diimine)] species [31], and [Pt(CH$_3$)$_4$(α-diimine)] [32]. Detailed investigations of the photochemistry of [Re(R)(CO)$_3$(dmb)] [26–29] and advanced quantum chemical calculations on model Mn and Re complexes [6–9,33–35] have demonstrated that the reaction occurs from a spin-triplet excited state of mixed SBLCT–MLCT character, in which the SBLCT component prevails. An intriguing difference between the photochemistry of methyl and ethyl complexes has been identified: Irradiation of [Re(Me)(CO)$_3$-(dmb)] produces radicals with a quantum yield of 0.4 (at 293 K), alongside the population of an unreactive trapping excited state that decays to the ground state with a lifetime of 30–40 ns [26]. A prominent dependence of the quantum yield on temperature reveals an activation barrier of ca. 1560 cm^{-1} on the reactive pathway. Photochemical radical formation does not occur at low temperatures

(< 195 K), at which only the trapping state is populated. This state was characterized by its emission and TRIR spectrum as having a ^{3}MLCT character with a significant SBLCT admixture [26]. Hereinafter, this state will be denoted ^{3}MLCT–SBLCT, to stress out its mixed character[1] [5]. On the other hand, homolysis of the Re–Et bond in [Re(Et)(CO)$_3$(dmb)] occurs with a temperature-independent quantum yield of unity. Radical products [Re(S)(CO)$_3$(dmb)]$^\bullet$ and Et$^\bullet$ are the only species observed on the nanosecond and longer timescales. They are formed even in low-temperature glasses [27].

A femto- and picosecond time-resolved spectroscopic study [11] of [Re(Me)(CO)$_3$(dmb)] and [Re(Et)(CO)$_3$(dmb)] has revealed the early excited state dynamics responsible for the photochemical Re–R bond homolysis and the reasons for the observed differences in photochemistry between the Me and Et complexes. The results are summarised in Fig. 5. Optical excitation of either complex populates an excited state of mixed ^{1}MLCT–SBLCT character. Ultrafast branching between radical formation through a dissociative ^{3}SBLCT–MLCT excited state and popula-

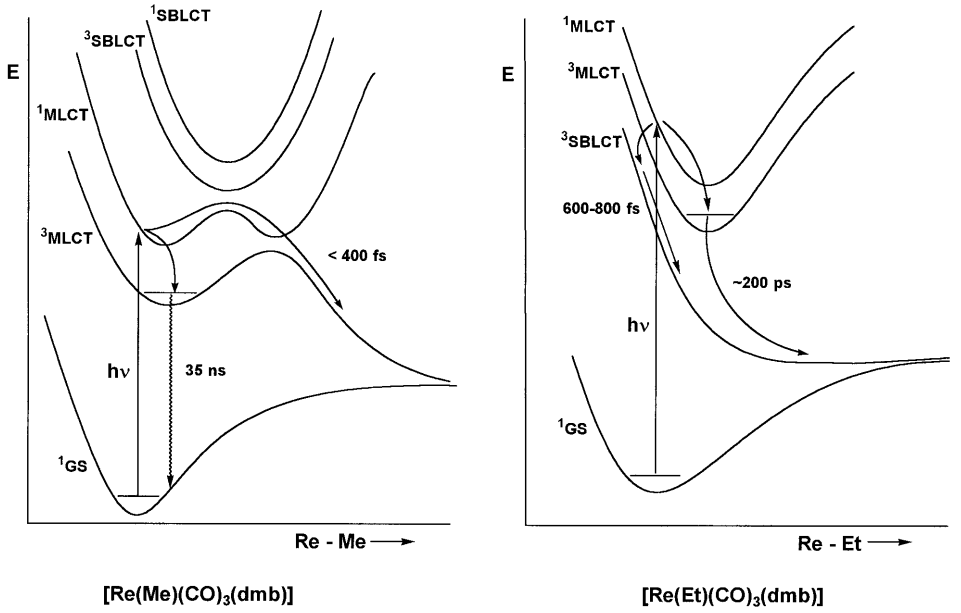

Fig. 5. Excited state dynamics of [Re(R)(CO)$_3$(dmb)]; R = Me, Et. Qualitative, idealised potential energy curves are used, which are based on curves calculated for the model complexes [Mn(H)(CO)$_3$(H–DAB)] and [Mn(Et)(CO)$_3$(H–DAB)] [6–8,33,47,48]. Only the principal characters of the exited states are indicated. Hence, MLCT and SBLCT correspond to MLCT–SBLCT and SBLCT–MLCT, respectively, used in the text. In reality, an extensive mixing between MLCT and SBLCT characters occurs [5,7,33,35].

[1] Similarly, a mixed notation SBLCT–MLCT will be used for SBLCT states which are, in [Re(R)(CO)$_3$(α-diimine)], strongly mixed with MLCT states [5].

tion of an unreactive ^{3}MLCT–SBLCT excited state occurs for both species, albeit with different rates: <400 fs for R = Me; 600–800 fs for R = Et. For [Re(Me)(CO)$_3$(dmb)], the reaction occurs on the potential energy surface of the optically prepared ^{1}MLCT–SBLCT state. Later along the Re–Me reaction coordinate this state acquires a dissociative ^{3}SBLCT–MLCT character via an intersystem crossing with an upper state of a predominant ^{3}SBLCT character, see Fig. 5. Theoretical calculations indicate [35] that spin–orbit coupling between MLCT and SBLCT states of different spin multiplicities is remarkably strong, up to 500 cm^{-1}, facilitating ^{1}MLCT$\rightarrow$^{3}SBLCT intersystem crossing. The, concurrently populated, unreactive ^{3}MLCT–SBLCT state is the lowest-energy excited state. Hence, its population prevents any Re–Me homolysis: it is a true trapping state. The quantum yield of Re–Me bond homolysis is thus determined by the branching ratio between the reactive and relaxation pathways.

The situation is profoundly different for [Re(Et)(CO)$_3$(dmb)], whose dissociative ^{3}SBLCT–MLCT state is the lowest excited state everywhere along the reaction coordinate. It is populated directly from the Franck–Condon state by ultrafast (600–800 fs) intersystem crossing, which now occurs close to the region of vertical excitation, parallel with population of the unreactive ^{3}MLCT–SBLCT state. Direct intersystem crossing of the Franck–Condon state into the ^{3}SBLCT–MLCT state leads to prompt radical formation. However, the behaviour of the ^{3}MLCT–SBLCT state is affected by the presence of the lower-lying ^{3}SBLCT–MLCT state. Instead of slowly decaying to the ground state, the ^{3}MLCT–SBLCT state decays very rapidly ($\tau = 213$ ps in CH_2Cl_2 or 83 ps in CH_3CN) into the energetically close, reactive ^{3}SBLCT–MLCT state, from which radicals are immediately formed. Population of the unreactive ^{3}MLCT–SBLCT state thus only delays the radical formation. Photochemical homolysis of a Re–Et bond in [Re(Et)(CO)$_3$(dmb)] thus occurs by two pathways: (i) a prompt route, which results from the population of the reactive state directly from the Franck–Condon state and which is completed within 600–800 fs; and (ii) a delayed pathway, which involves the population of an intermediate ^{3}MLCT–SBLCT state which decays into the lower-lying reactive state with a time constant of about 200 ps. It follows that the differences in the photochemical behaviour of the Me and Et complexes arise from the different ordering of the Franck–Condon (^{1}MLCT–SBLCT), reactive (^{3}SBLCT–MLCT) and trapping (^{3}MLCT–SBLCT) excited states and from different shapes of their potential energy surfaces.

The reactive ^{3}SBLCT–MLCT excited state is derived from mixed $\sigma_{Re-R} \rightarrow \pi^*$ and $d_{xz} \rightarrow \pi^*$ excitations [4–9]. Its potential energy curve is unbound along the Re–R coordinate, presumably due to an interaction with a strongly dissociative $\sigma\sigma^*$ state. In an orbital picture, this interaction amounts to the increasing population of the highly antibonding d_{z^2} orbital and its mixing with the π^*(bpy) orbital, which occurs as the Re–R bond elongates [8].

Interestingly, the actual shape and character of the ^{3}SBLCT potential energy curve, and hence, the dynamics of bond splitting, sensitively depend on the molecular structure and even the medium. Thus, photochemical Re–R (R = Et, ^{i}Pr,

benzyl) bond homolysis is much slower for analogous [Re(R)(CO)$_3$(^{i}Pr–DAB)] complexes in hydrocarbon solutions ($\tau = 60-250$ ns, depending on R). However, even [Re(R)(CO)$_3$(^{i}Pr–DAB)] complexes undergo ultrafast Re–R bond homolysis in coordinating or polar solvents [36,37].

4. LLCT photochemistry: dissociative isomerisation of *fac*-[Mn(Br)(CO)$_3$(^{i}Pr–DAB)]

The lowest allowed electronic transition of *fac*-[Mn(X)(CO)$_3$(^{i}Pr–DAB)]; X = halide; complexes has a mixed X → DAB LLCT and Mn → DAB MLCT character due to strong mixing between the Mn d_{xz} and halide p_x orbitals in which the transition originates. The relative contribution of the LLCT component increases in the order X = Cl < Br < I. Irradiation into the lowest absorption band of *fac*-[Mn(X)(CO)$_3$(^{i}Pr–DAB)] produces complexes with the halide ligand in the equatorial position [38,39]. In non-coordinating solvents, this reaction looks like a simple photochemical isomerisation:

$$fac\text{-}[Mn(X)(CO)_3(^i\text{Pr–DAB})] \xrightarrow{h\nu} mer\text{-}[Mn(X)(CO)_3(^i\text{Pr–DAB})] \quad (2)$$

Formation of a substituted bis-carbonyl product in coordinating solvents (pyridine, THF) or in the presence of Lewis bases (phosphines, phosphites) clearly shows [38] that this isomerisation involves a dissociation of a CO ligand:

$$fac\text{-}[Mn(X)(CO)_3(^i\text{Pr–DAB})] \xrightarrow{h\nu,\ S} cis,cis\text{-}[Mn(X)(S)(CO)_2(^i\text{Pr–DAB})] + CO \quad (3)$$

The halide ligand in the photoproduct lies in the equatorial Mn(DAB) plane. Similar dissociative substitution has been observed [40] for [Ru(I)(Me)(CO)$_2$(dmb)].

The reaction mechanism of the dissociative substitution of *fac*-[Mn(Br)(CO)$_3$-(^{i}Pr–DAB)], established [12] by ultrafast time-resolved absorption spectroscopy, is shown in Fig. 6. The CO dissociation step is surprisingly slow, occurring with a time constant of 11 ps. A second step, attributed to a relaxation of the CO-loss primary product, follows with a time constant of 22 ps. Presumably, this step involves a full coordination of the solvent molecule and an accommodation of the Br^- ligand in its equilibrium position in the equatorial molecular plane, together with full vibrational relaxation.

The CO dissociation from *fac*-[Mn(X)(CO)$_3$(^{i}Pr–DAB)] is remarkably slow, especially in comparison with femtosecond rates observed [10,41] for [Cr(CO)$_4$-(bpy)] or Cr(CO)$_6$ whose CO photodissociation reactions occur on unbound excited state potential energy surfaces. This comparison suggests that a different mechanism operates for *fac*-[Mn(X)(CO)$_3$(^{i}Pr–DAB)]. Indeed, a quantum chemical study of the excited state potential energy surfaces of *fac*-[Mn(Cl)(CO)$_3$(H–DAB)] has shown [42] that all low-lying excited states have well-developed minima and, hence, profound energy barriers along both equatorial and axial Mn–CO reaction coordinates. These barriers are lower, but still significant, event if the concurrent movement of the halide ligand is included in the calculation. However, the

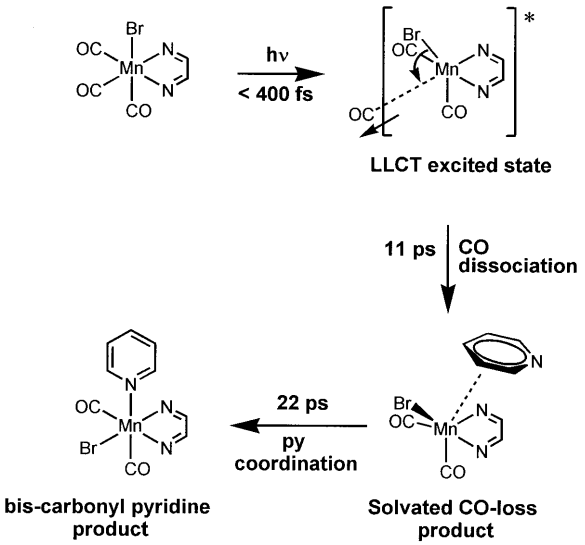

Fig. 6. The mechanism of the photochemical dissociative substitution of *fac*-[Mn(Br)(CO)$_3$(^{i}Pr–DAB)].

calculations indicate that the bound potential energy curve of the LLCT excited state is partly 'immersed' into the energy well formed by the ground state potential energy curve along the reaction coordinate which includes equatorial Mn–CO bond dissociation, together with bending of the halide ligand toward the equatorial plane. This is shown schematically in Fig. 7. In such a situation, a continuum of dissociative states exists above the maximum of the energy barrier on the ground state potential energy surface. For some energy values, resonance coupling occurs between the vibrational levels of the electronically excited state and the dissociative ground state continuum. It was suggested [42] that this coupling can provide a pathway for CO dissociation, concerted with the movement of the axial halide ligand toward the vacated equatorial position. Such a process is slower than smooth CO dissociation on an unbound potential energy surface, for example, as occurs for [Cr(CO)$_4$(bpy)] or Cr(CO)$_6$.

5. Ultrafast metal–ligand bond splitting upon MLCT excitation of carbonyl-diimine complexes

The three examples discussed above epitomise three different mechanisms whereby excitation into MLCT and related excited states can induce splitting of metal–ligand bonds. The dissociative isomerisation of [Mn(Br)(CO)$_3$(^{i}Pr–DAB)] represents a rather special mechanism, whereby resonant coupling with the dissociative continuum of the electronic ground state is enabled by a particular geometry of ground- and excited-state potential energy surfaces [42]. On the other hand, CO dissociation from [Cr(CO)$_4$(bpy)] and alkyl homolysis from [Re(R)(CO)$_3$(dmb)] occur on dissociative potential energy surfaces.

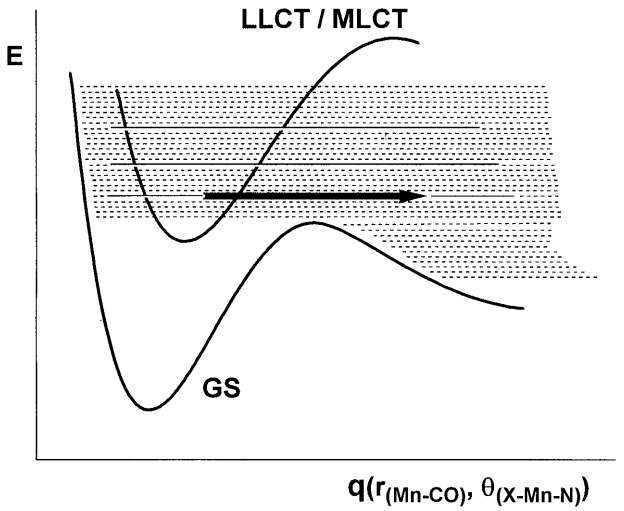

Fig. 7. Resonance coupling between a reactive excited state and the dissociative continuum of an electronic ground state, relevant to the primary step of the photochemical dissociative isomerisation of [Mn(Br)(CO)$_3$(^{i}Pr–DAB)]. The reaction coordinate includes both the equatorial Mn–CO distance and the angle between the Mn–Br bond and the equatorial, i.e. Mn(DAB), molecular plane.

In general, it appears that two concurrent pathways are open for optically prepared CT excited states of reactive organometallic molecules: relaxation to trapping excited states and bond splitting, the latter occurring either directly from a spin-singlet MLCT state (CO dissociation) or after intersystem crossing to a triplet excited state (Re–R homolysis). The quantum yield of the bond splitting reaction is determined by the corresponding branching ratio. Obviously, the energetic order of the Franck–Condon, reactive, and trapping excited state(s) is of crucial importance.

The charge transfer excited states responsible for CO dissociation or bond homolysis acquire their dissociative character by interaction (avoided crossing) with high-lying strongly repulsive states of LF or $\sigma\sigma^*$ origin, respectively [6–9,20,21,33]. Depending on the detailed character and geometry of the potential energy surfaces along the reaction coordinate, this interaction can produce either an energy barrier on the reactive potential energy surface (Fig. 8-left) or it can lead to a flat, dissociative surface (Fig. 8, right). Now, an interesting question arises, whether the reaction proceeds as a smooth evolution on the same potential energy surface which gradually changes its character by mixing with higher excited state(s) or whether a 'state crossing' to a dissociative (LF or $\sigma\sigma^*$) excited state occurs at some point along the reaction coordinate. At first glance, this may seem to be just a semantic question. However, these two possibilities are physically very different: state crossing is a non-adiabatic process, which occurs with a probability less than unity, thus limiting the quantum yield. On the other hand, smooth evolution on a dissociative surface is adiabatic, occurring with a unit probability [43]. In the first

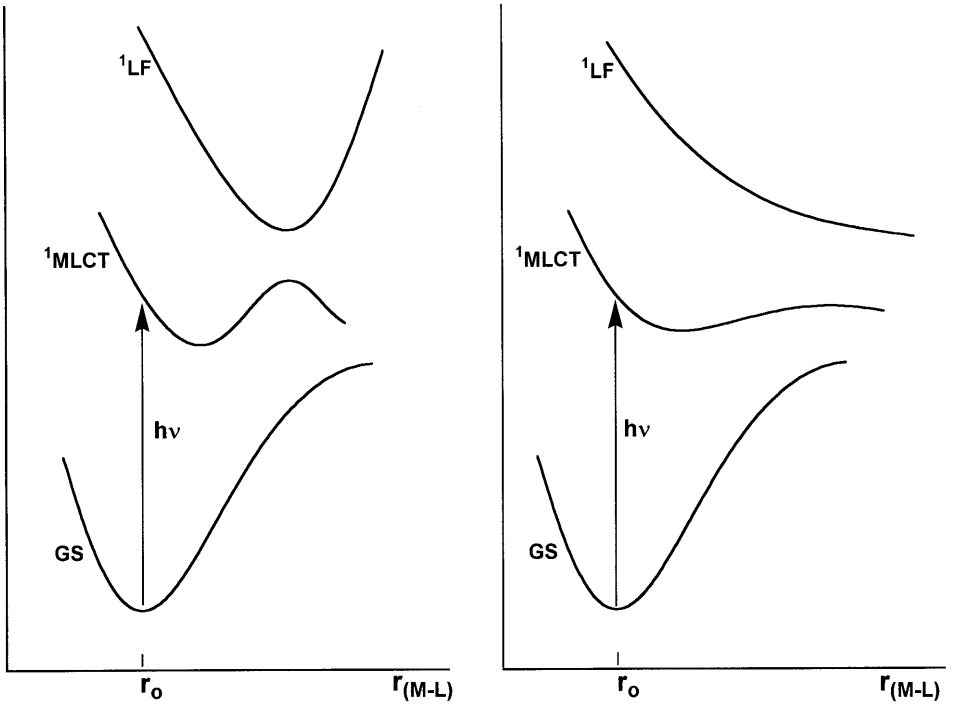

Fig. 8. Possible shapes of MLCT potential energy curves which become dissociative by interaction with an upper, strongly repulsive LF state. Note that this interaction gradually changes the character of the states involved along the reaction coordinate. The state description as MLCT, LF, etc. is thus valid only at the geometry of the Franck–Condon (vertical) excitation. These diagrams can be generalised to other types of excited states.

approximation, these two cases, shown schematically in Fig. 9, may be distinguished using the Landau–Zerner equation (4) for the probability (P) of a nonadiabatic transition occurring between the two states [43]:

$$P = 1 - \exp(-\pi\gamma/2) \tag{4a}$$

$$\gamma = \tau \frac{H}{\hbar} = \frac{H^2}{\hbar v |F_2 - F_1|} \tag{4b}$$

where H stands for the interaction energy between the two states, τ is the time which the reacting system spends in the crossing region, v is the frequency with which the system passes through the crossing region, and F_1 and F_2 are the slopes of the potential energy curves of the two states at the point of their crossing.

Essentially, the state crossing mechanism requires small values of γ. This will happen for transitions between weakly coupled states whose potential energy surfaces cross at sharp angles. A simple estimate shows that a 300 fs process will be adiabatic ($P \geq 0.99$) when the coupling between electronic states is larger than

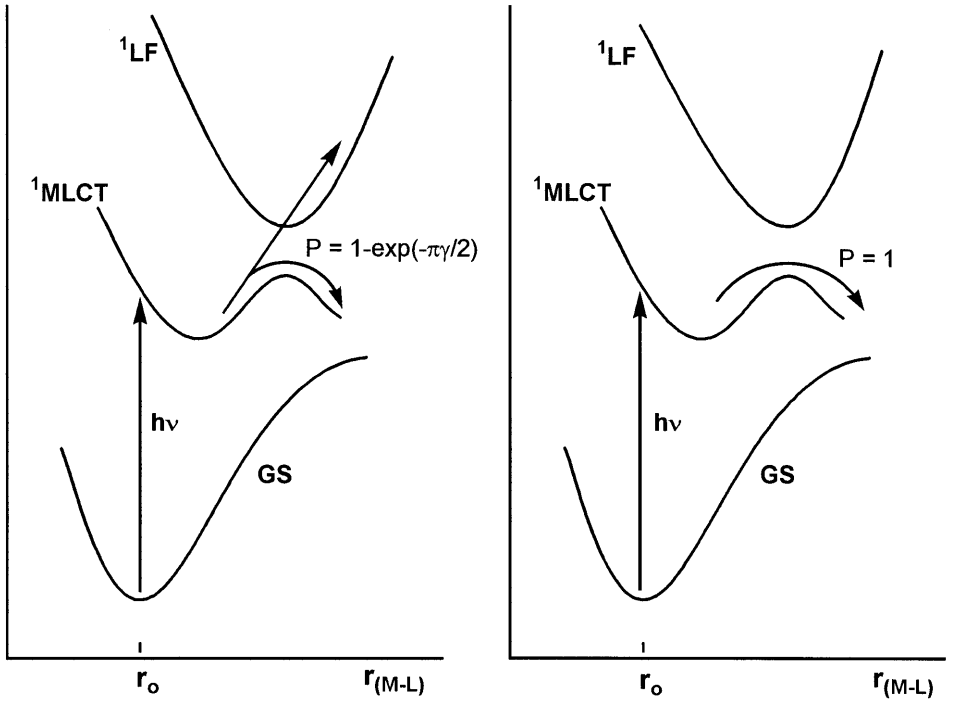

Fig. 9. Adiabatic and nonadiabatic excited state processes. Left: nonadiabatic crossing between a bound MLCT and dissociative LF state. Right: adiabatic evolution on a single potential energy curve which acquires dissociative character by interaction with an upper state. These diagrams can be generalised and applied to other types of excited states.

about 50 cm^{-1}. Quantum chemical calculations on model Mn carbonyl-diimine complexes or $[Cr(CO)_4(bpy)]$ [8,9,20,34] give coupling values of hundreds or even thousands of wavenumbers. Evidently, we may conclude that most of the reactions of CT excited states occur as adiabatic, smooth evolutions on potential energy surfaces of single excited states that gradually change their character along the reaction path by interactions with other excited states. These interactions can modify the shape of the reactive state potential energy surface and make it dissociative. A crossing to another, repulsive, state does not appear to be involved as a distinct mechanistic step in the cases of photochemical CO dissociation or alkyl homolysis from organometallic carbonyl-diimine complexes.

Population of trapping excited state(s) occurs in most cases directly from the Franck–Condon excited state, concurrently with bond splitting. This initial branching of the optically prepared excited state is best described by wave packet dynamics on realistic potential energy surfaces. Structural factors which determine the branching ratio as well as effects of reaction conditions (temperature, solvent, pressure) on quantum yields of ultrafast photochemical reactions still remain to be understood. The importance and wide occurrence of the branching of wave packet evolution between reactive and relaxation pathways is underlined by the observa-

tion that it also limits the quantum yields of the photochemical generation of catalytically important, coordinatively unsaturated intermediates implicated in photochemical C–H bond activation [44–46].

6. Conclusions

1. Early excited state dynamics that occur from a few tens of femtoseconds until (at most) a few hundreds of picoseconds after excitation largely determine the overall outcome of organometallic photochemical reactions. Branching of the evolution of an optically prepared Franck–Condon state between bond splitting and relaxation to unreactive states is a general mechanism that limits photochemical quantum yields.
2. MLCT excited states can become dissociative (unbound) with respect to the splitting of an axial M–CO bond by interacting with a higher-lying, strongly dissociative LF state(s), that occurs along the reaction coordinate. Dissociation of a CO ligand then proceeds promptly (in a few hundreds of fs) after optical excitation, following a smooth adiabatic evolution on the potential energy surface of the optically prepared, spin-singlet Franck–Condon state. The metal–alkyl bond homolysis observed in organometallic carbonyl-diimine complexes occurs from a ^{3}SBLCT state (usually with some admixed MLCT character). This state becomes dissociative by interaction with a $^3\sigma\sigma^*$ state along the reaction coordinate.
3. Organometallic photochemistry cannot be interpreted by considering only the orbitals depopulated and populated in optical excitations. Instead, relative positions and energy ordering of Franck–Condon, dissociative, and unreactive ('trapping') excited states, as well as their interactions and orbital mixing along possible reaction coordinates should be taken into account. Interactions between excited states and the ground state can also be important. A close interplay between experiment and theory is essential.

Acknowledgements

A long-term collaboration with Professor D.J. Stufkens (Universiteit van Amsterdam) and Dr C. Daniel on experimental and theoretical aspects of organometallic photochemistry is gratefully appreciated. Dr P. Matousek and Dr T. Parker (CLF, Rutherford Appleton Laboratory) are thanked for their help with the ultrafast experiments. Dr C.J. Kleverlaan is acknowledged for his contribution to the study of Re–R bond homolysis.

References

[1] A. Vogler, H. Kunkely, Coord. Chem. Rev. 177 (1998) 81.
[2] A. Vlček Jr., Coord. Chem. Rev. 177 (1998) 219.

[3] A. Vogler, H. Kunkely, Coord. Chem. Rev. 171 (1998) 399.
[4] D.J. Stufkens, A. Vlček Jr., Coord. Chem. Rev. 177 (1998) 127.
[5] D. Guillaumont, M.P. Wilms, C. Daniel, D.J. Stufkens, Inorg. Chem. 37 (1998) 5816.
[6] K. Finger, C. Daniel, J. Am. Chem. Soc. 117 (1995) 12322.
[7] D. Guillaumont, C. Daniel, Coord. Chem. Rev. 177 (1998) 181.
[8] D. Guillaumont, C. Daniel, J. Am. Chem. Soc. 121 (1999) 11733.
[9] D. Guillaumont, C. Daniel, in preparation.
[10] I.R. Farrell, P. Matousek, A. Vlček Jr., J. Am. Chem. Soc. 121 (1999) 5296.
[11] I.R. Farrell, P. Matousek, C.J. Kleverlaan, A. Vlček, Jr., Chem. Eur. J. (2000) in press.
[12] I.R. Farrell, P. Matousek, A. Vlček, Jr., Inorg. Chem. (1999) submitted for publication.
[13] R.W. Balk, T. Snoeck, D.J. Stufkens, A. Oskam, Inorg. Chem. 19 (1980) 3015.
[14] S. Wieland, K.B. Reddy, R. van Eldik, Organometallics 9 (1990) 1802.
[15] W.F. Fu, R. van Eldik, Inorg. Chim. Acta 251 (1996) 341.
[16] W.-F. Fu, R. van Eldik, Inorg. Chem. 37 (1998) 1044.
[17] J. Víchová, F. Hartl, A. Vlček Jr., J. Am. Chem. Soc. 114 (1992) 10903.
[18] I.G. Virrels, M.W. George, J.J. Turner, J. Peters, A. Vlček Jr., Organometallics 15 (1996) 4089.
[19] D. Guillaumont, C. Daniel, A. Vlček Jr., Inorg. Chem. 36 (1997) 1684.
[20] D. Guillaumont, C. Daniel, A. Vlček, Jr., J. Phys. Chem. A, in press.
[21] A. Vlček Jr., J. Víchová, F. Hartl, Coord. Chem. Rev. 132 (1994) 167.
[22] H.K. van Dijk, D.J. Stufkens, A. Oskam, J. Am. Chem. Soc. 111 (1989) 541.
[23] C.E. Johnson, W.C. Trogler, J. Am. Chem. Soc. 103 (1981) 6352.
[24] W.C. Trogler, in: A.B.P. Lever (Ed.), Excited States and Reactive Intermediates. ACS Symposium Series 307, American Chemical Society, Washington, DC, 1986, p. 177.
[25] S. Záliš, C. Daniel, A. Vlček, Jr., J. Chem. Soc. Dalton Trans. (1999) 3081.
[26] C.J. Kleverlaan, D.J. Stufkens, I.P. Clark, M.W. George, J.J. Turner, D.M. Martino, H. van Willigen, A. Vlček Jr., J. Am. Chem. Soc. 120 (1998) 10871.
[27] C.J. Kleverlaan, D.J. Stufkens, Inorg. Chim. Acta 284 (1999) 61.
[28] C.J. Kleverlaan, D.M. Martino, J. van Slageren, H. van Willigen, D.J. Stufkens, A. Oskam, Appl. Magn. Reson. 15 (1998) 203.
[29] C.J. Kleverlaan, D.M. Martino, H. van Willigen, D.J. Stufkens, A. Oskam, J. Phys. Chem. 100 (1996) 18607.
[30] B.D. Rossenaar, D.J. Stufkens, A. Oskam, J. Fraanje, K. Goubitz, Inorg. Chim. Acta 247 (1996) 215.
[31] D.J. Stufkens, M.P. Aarnts, B.D. Rossenaar, A. Vlček Jr., Pure Appl. Chem. 69 (1997) 831.
[32] S. Hasenzahl, H.-D. Hausen, W. Kaim, Chem. Eur. J. 1 (1995) 95.
[33] D. Guillaumont, K. Finger, M.R. Hachey, C. Daniel, Coord. Chem. Rev. 171 (1998) 439.
[34] K. Finger, C. Daniel, P. Saalfrank, B. Schmidt, J. Phys. Chem. 100 (1996) 3368.
[35] C. Daniel, D. Guillaumont, C. Ribbing, B. Minaev, J. Phys. Chem. A 103 (1999) 5766.
[36] B.D. Rossenaar, M.W. George, F.P.A. Johnson, D.J. Stufkens, J.J. Turner, A. Vlček Jr., J. Am. Chem. Soc. 117 (1995) 11582.
[37] B.D. Rossenaar, C.J. Kleverlaan, M.C.E. van de Ven, D.J. Stufkens, A. Vlček Jr., Chem. Eur. J. 2 (1996) 228.
[38] G.J. Stor, S.L. Morrison, D.J. Stufkens, A. Oskam, Organometallics 13 (1994) 2641.
[39] C.J. Kleverlaan, F. Hartl, D.J. Stufkens, J. Photochem. Photobiol. A Chem. 103 (1997) 231.
[40] C.J. Kleverlaan, D.J. Stufkens, J. Photochem. Photobiol. A 116 (1998) 109.
[41] T. Lian, S.E. Bromberg, M.C. Asplund, H. Yang, C.B. Harris, J. Phys. Chem. 100 (1996) 11994.
[42] A. Rosa, G. Ricciardi, E.J. Baerends, D.J. Stufkens, J. Phys. Chem. 100 (1996) 15346.
[43] H. Frauenfelder, P.G. Wolynes, Science 229 (1985) 337.
[44] S.E. Bromberg, T. Lian, R.G. Bergman, C.B. Harris, J. Am. Chem. Soc. 118 (1996) 2069.
[45] S.E. Bromberg, H. Yang, M.C. Asplund, T. Lian, B.K. McNamara, K.T. Kotz, J.S. Yeston, M. Wilkens, H. Frei, R.G. Bergman, C.B. Harris, Science 278 (1997) 260.
[46] J.B. Asbury, H.N. Ghosh, J.S. Yeston, R.G. Bergman, T. Lian, Organometallics 17 (1998) 3417.
[47] K. Finger, C. Daniel, J. Chem. Soc. Chem. Commun. (1995) 1427.
[48] D. Guillaumont, PhD Thesis, Laboratoire de Chimie Quantique CNRS UMR 7551 et Université Louis Pasteur, Strasbourg, France, 1998, p. 166.